JOURNAL OF APPLIED ELECTROCHEMISTRY 16 (1986) 555–564

The estimation of the residual capacity of sealed lead–acid cells using the impedance technique

M. HUGHES, R. T. BARTON, S.A.G.R. KARUNATHILAKA, N.A. HAMPSON

Chemistry Department, University of Technology, Loughborough, Leicestershire LE11 3TU, UK

Received 7 June 1985; revised 23 July 1985

The problem of estimating the residual usable energy of a lead–acid cell has been intensified by the introduction of fully sealed units. These rely on the recombination of gaseous oxygen produced during overcharge at the positive electrode with the active material at the negative electrode. This introduction has removed the possibility of electrolyte density measurements, third electrode measurements and restricted residual capacity assessments to the two cell terminals. A method for this process is described using a parameter based on a characteristic frequency. The parameter is also a useful measure of cell ageing.

Nomenclature

R_{SOL}	Ohmic resistance of cell (Ω)
θ	Charge-transfer resistance of positive and negative electrodes (Ω)
CL	Double-layer capacitance of both positive and negative electrodes (F)
σ	Warburg diffusion ($\Omega s^{-1/2}$)
C_{EXT}	External series capacitor in analogue Fig. 5 (F)
R_{EXT}	External resistor in parallel with C_{EXT} in the anologue circuit Fig. 5 (Ω)
IND	Inductor in Fig. 5 representing the geometrical effects of the cell at high frequencies (Henries)
R_{IND}	External resistor in parallel with IND in the analogue circuit Fig. 5 (Ω)
γ	Roughness factor allowing for the porosity of both electrodes

1. Introduction

During the past decade a number of investigations of state-of-charge [1] and residual capacity [2] have been made. These have generally been successful in the case of primary cells.

The generally used method is the impedance technique where a relatively simple harmonic frequency test sequence is sufficient to estimate residual capacity within limits generally acceptable to the user. An example of this is our work with the HgO/KOH/Zn cell where the estimation of the charge-transfer resistance using a high and intermediate frequency harmonic test yielded the residual capacity [3].

The Ni/Cd secondary cell has been the subject of a number of papers [4]. The impetus for this has been the lack of change of electrolyte density (and therefore cell open circuit potential) during the course of the discharge. The impedances of Ni/Cd cells as functions of the residual capacity have been intensively studied by us [5] and others [4]. Within the linear polarization region ($\Delta V \sim 7$ mV) the shape of the impedance spectrum of the Ni/Cd cells did not change appreciably with the residual charge. It should be noted that there are statements in the literature to the effect that at a sufficiently low frequency the impedance could be used to assess residual charge. We have found such measurements not to be particularly effective and we now consider that the earlier works might well have been complicated by non-electrochemical artefacts of the type encountered by ourselves [6]. A parallel investigation was recently launched using a potential step somewhat outside the linear region [5]. This approach has shown considerable promise; however, it is not as yet possible to provide a satisfactory theoretical background for the effects observed.

0021–891X/86 $03.00 + .12

With the introduction of the fully sealed lead–acid cell the need for a method of residual capacity detection became quite important. It has long been established that an accurate electrolyte density measurement coupled with a cell voltage reading provided a reasonable indication of residual capacity. With the fully sealed cell the first of these was clearly not possible. In any case it was desirable to have an indication of the 'state-of-health' of the lead–acid cell which was indicative of the state of the electrodes rather than the electrolyte. We decided therefore to investigate the frequency response of lead–acid cells in order to establish the possibility of providing a suitable test of residual capacity and state-of-health.

A number of papers on the impedance of lead and lead overlayed with PbO_2 have been published from this laboratory [7]. From this work it was clear that there is a high frequency region where a charge-transfer semicircle could be distinguished. Indeed on driving the PbO_2 (positive) electrode more negative the charge-transfer semicircle changes in dimensions. These experiments were potentiostatic in as much as the potential was shifted abruptly and the experiment made as rapidly as possible with the apparent electrode potential constant in the presence of a growing $PbSO_4$ layer at the electrode. Clearly the shortcoming in the experiments was that the flow of d.c. at potentials negative of the equilibrium would progressively cover the electrode with $PbSO_4$. The introduced quite unquantifiable complications, indeed the sign of the slope d log θ/dE was of the wrong sign. This was interpreted as a progressive blocking of the electrode by $PbSO_4$ which reduced the reacting area of the electrode and in effect engendered an apparent reduction in θ. Kelly [8] was able to find the true potential dependence of the charge-transfer reaction by correcting the experimental θ for the area factor using the double-layer capacitance.

In this work the circuit elements of the electrode analogue network were obtained by the mathematical decomposition of the electrode impedance using the technique developed by Karunathilaka *et al.* [9]. Clearly if such information is useful for the residual capacity estimation a more facile way of obtaining it is required than using a large computer. Nevertheless it was considered worthwhile to embark upon an investigation of the impedance of fully sealed cells (2.5 A h) manufactured using the rolled-up format. This paper describes the results.

2. Experimental procedure

Experiments were carried out as described previously [10]. However, the correction for the complex nature of the interface (Solatron 1170) calibration impedance was applied in view of the low impedance of the cells [6].

Two types of 2.5 A h fully sealed lead–acid cells were used, the first group were manufactured during 1977 and the second group were purchased during 1984. The older cells were considered to have stabilized and were therefore investigated after capacity estimation at the 0.05 C rate. The new cells were cycled at the 0.05 C rate in order to bring them to some measure of stabilized condition. This was not achieved as readily as would have been expected for flooded technology cells, The reluctance to yield the rated nominal capacity could equally be due to local variations in manufacturers processing. When the capacities were in excess of nominal and reasonably stable impedance measurements were commenced.

Impedance data were displayed as complex plane plots and read into the computer (Honeywell/Multics Software) in order to apply the decomposition program.The data were ultimately matched to an analogue containing elements for the positive and negative electrodes lumped together as one conversion [1] with allowances for inherent geometrical inductance, electrolyte and connector resistances. The porous nature of the positive was recognized in our modelling by the squaring procedure [11] applied to the positive electrode which in the range down to about 5 mHz could be represented by a simple Randles connection [2]. The lead sulphate which develops on reaction was best dealt with as a parallel combination of resistance and capacitance. The argument behind this procedure has been the recognition of the (approximate) equivalent magnitudes of the impedances of the positive and negative lead–

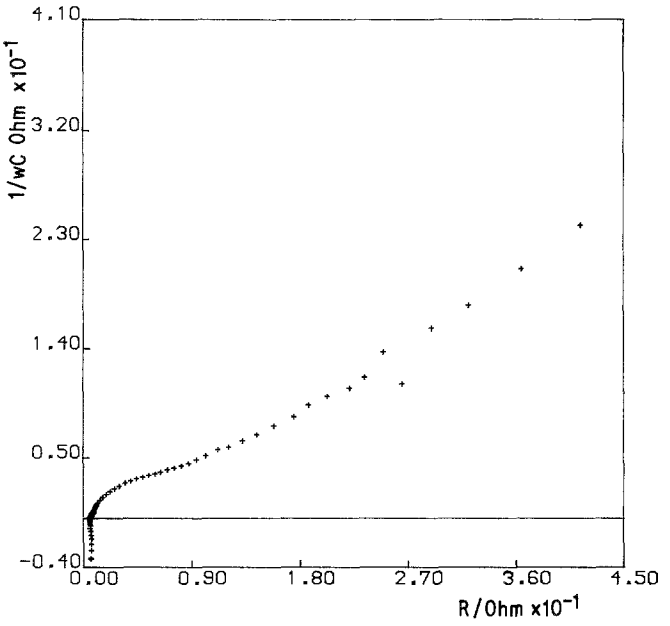

Fig. 1. Impedance spectrum of a fully charged 2.5 A h lead–acid cell in the frequency range 60 kHz to 1 mHz. Ten points per decade.

acid electrodes and since the combination of the electrode impedances involves a simple material addition of linear elements the 'lumped cell' procedure appears to us the simplest way forward.

3. Results and discussion

The impedance of a fully charged cell is shown in Fig. 1. The locus consists of an inductive region at high frequency which curves over to form a Warburg type tail. This tail changes shape from 45° to a somewhat lower dihedral. This is possibly due to the porosity effect, the porous nature of the electrode being revealed at the lower frequency. The locus joins the real axis (at $\omega = \infty$) at 90° indicating that the electrode is behaving as a planar electrode. The Randles representation of the impedance shows the resistive component lying below the capacitive component which is

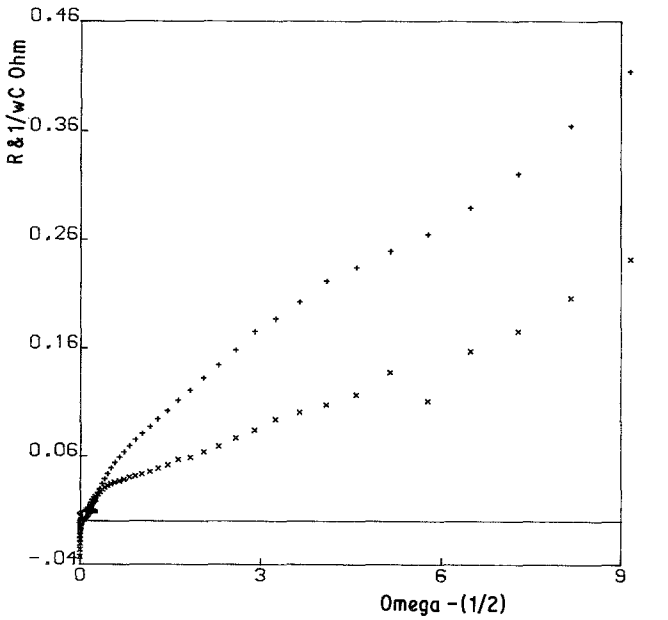

Fig. 2. Randles representation of the cell impedance shown in Fig. 1. (+) Resistive component and (x) capacitive component.

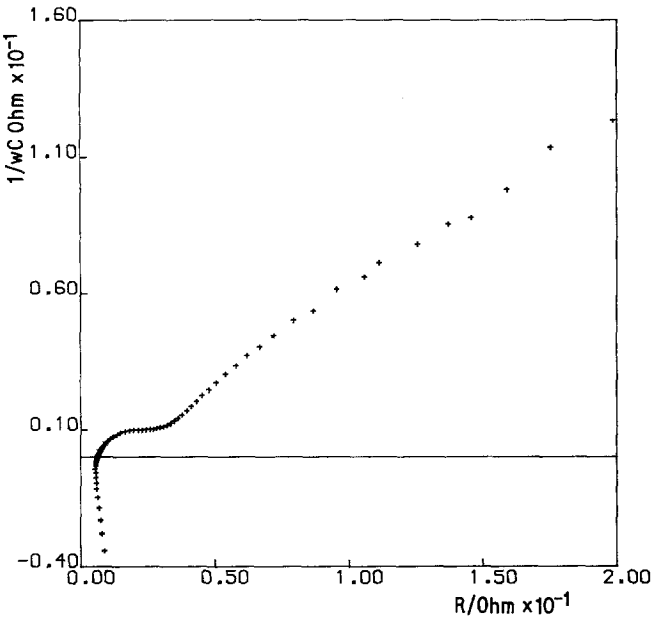

Fig. 3. Impedance spectrum of a fully sealed lead–acid cell 90% state-of-charge in the frequency range 60 kHz to 1 mHz. Ten points per decade.

indicative of adsorption in the sense of Randles and Laitinen [12]. This is illustrated in Fig. 2 and has been discussed by us previously [13].

The impedance plot of a cell containing 90% residual capacity is shown in Fig. 3. Here the high frequency semicircle is well developed and tails off to a Warburg line which changes slope to a linear dihedral illustrating again a common feature of the frequency response of these cells. The impedance plots at lower residual capacities resembled Fig. 3 throughout the range to zero capacity. The representation of the impedance components displayed against $\omega^{-1/2}$ were all typified by Fig. 4 which showed the relocation due to the double-layer effects followed by two approximately parallel lines similar to a simple Randles conversion. At the lower frequency end of the experimental range the in-phase and out-

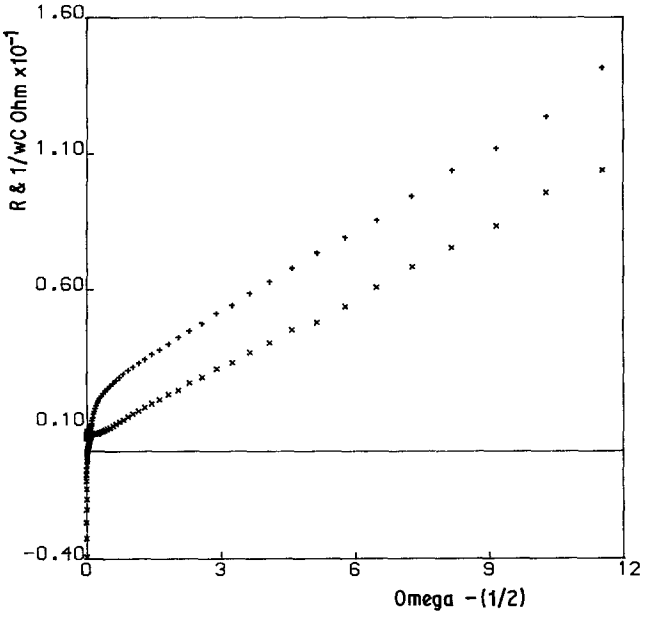

Fig. 4. Randles plot of a 2.5 A h lead–acid cell 80% state-of-charge in the frequency range 60 kHz to 1 mHz. (+) Resistive component, (x) capacitive component.

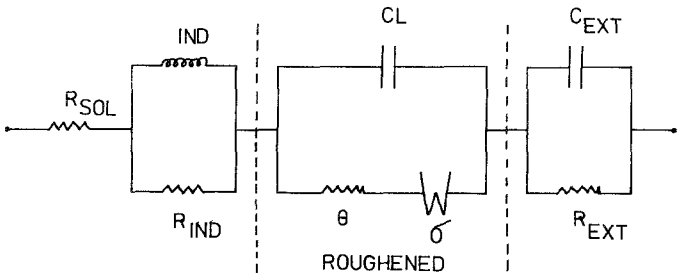

Fig. 5. Analogue circuit used to describe the impedance of the 2.5 A h fully sealed lead–acid cell.

of-phase lines diverged slightly in keeping with the porosity effect on the Warburg Slope.

The general shapes of the impedance loci representing all cells tested irrespective of age were similar to those already described.

The decomposition of the complex impedance pattern was carried out as described previously using the model conforming to the analogue shown in Fig. 5. In all cases the decomposition was satisfactorily accomplished and Tables 1, 2 and 3 show the values of the circuit elements conforming to the various residual capacities (the parameters are defined in the Nomenclature).

3.1. *The identification of a residual charge parameter*

It was clear that the components of the cell analogue do not change smoothly and consistently

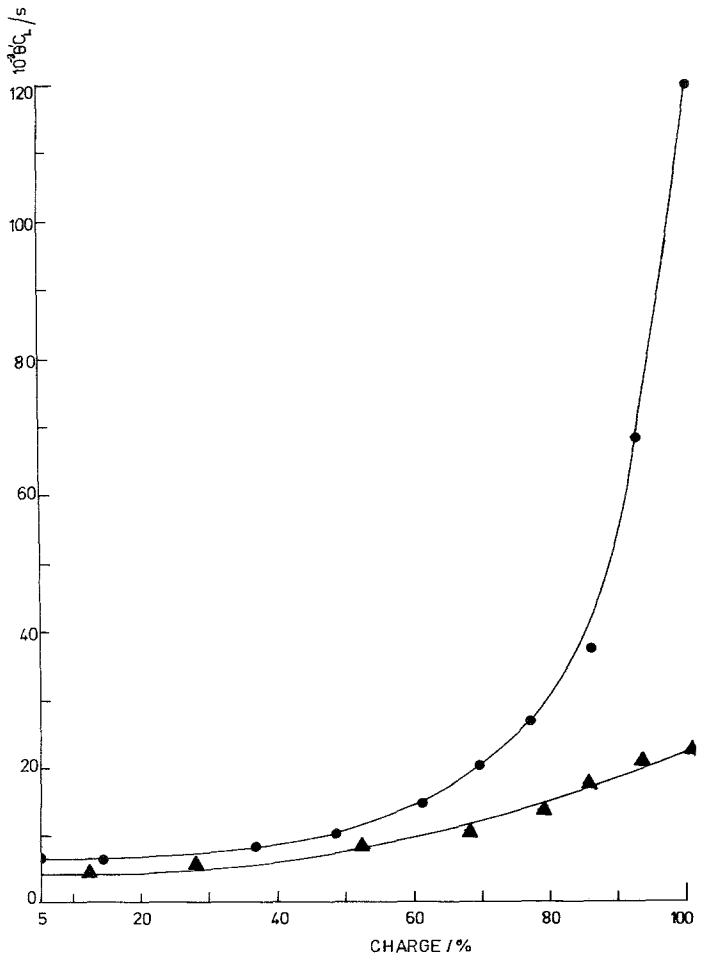

Fig. 6. Relationship of $\theta' C_L$ to residual capacity for the (●) new and (▲) old cells from the data obtained using the analogue circuit shown in Fig. 5.

Table 1. Values of computed circuit components for a new cell

Residual capacity (%)		R_{SOL} (Ω)	θ (Ω)	*CL (F)*	σ ($\Omega s^{-1/2}$)	γ	C_{EXT} *(F)*	R_{EXT} (Ω)	*IND (H)*	R_{IND} (Ω)	*Error* (±)
1.24	R†	3.46×10^{-2}	7.94×10^{-4}	0.18	1.21×10^{-2}	0.5	1×10^{12}*	1×10^{10}*	7.83×10^{-8}	1×10^{10}*	2.3×10^{-3}
	C†	3.46×10^{-2}*	7.94×10^{-4}*	0.18	1.21×10^{-2}*	0.5	1×10^{-12}*	1×10^{10}*	7.83×10^{-8}	1×10^{10}*	2.31×10^{-3}
9.37	R	1.48×10^{-2}	4.63×10^{-3}	0.44	1.00×10^{-2}	0.83	1078*	1×10^{10}*	9.20×10^{-8}	1×10^{10}*	9.8×10^{-4}
	C	1.48×10^{-2}	1.98×10^{-3}	1.82	6.35×10^{-3}	0.74	1078	1×10^{10}*	9.24×10^{-8}	1×10^{10}*	8.05×10^{-4}
27.64	R	7.49×10^{-3}	8.31×10^{-4}	3.07	3.58×10^{-3}	0.76	3639*	1×10^{10}*	1.00×10^{-7}*	1×10^{10}*	6.28×10^{-4}
	C	7.49×10^{-3}*	8.85×10^{-4}	2.21	3.47×10^{-3}	0.78	3639	1×10^{10}*	1.00×10^{-7}	1×10^{10}*	4.41×10^{-4}
23.92	R	8.64×10^{-3}	1.74×10^{-3}	4.33	3.84×10^{-3}	0.77	2101*	1×10^{10}*	9.94×10^{-8}*	1×10^{10}*	7.58×10^{-4}
	C	8.64×10^{-3}*	3.18×10^{-4}	16.21	1.79×10^{-3}	0.64	2101	1×10^{10}*	9.94×10^{-8}	1×10^{10}*	4.56×10^{-4}
41.97	R	6.45×10^{-3}	5.61×10^{-3}	1.72	6.96×10^{-3}	0.87	2702*	1×10^{10}*	1.10×10^{-7}	1×10^{10}*	8.52×10^{-4}
	C	6.45×10^{-3}*	2.08×10^{-3}	4.96	4.50×10^{-3}	0.74	2702	1×10^{10}*	1.10×10^{-7}	1×10^{10}*	7.93×10^{-4}
52.36	R	4.51×10^{-3}	7.12×10^{-3}	0.98	8.23×10^{-3}	0.82	5851*	1×10^{10}*	9.11×10^{-8}*	1×10^{10}*	6.03×10^{-4}
	C	4.51×10^{-3}*	3.21×10^{-3}	2.52	6.08×10^{-3}	1.0*	5851	1×10^{10}*	9.11×10^{-8}	1×10^{10}*	3.65×10^{-4}
65.91	R	5.17×10^{-3}	1.13×10^{-2}	0.59	1.24×10^{-2}	1.0*	2.4×10^{13}*	1×10^{10}*	9.16×10^{-8}*	1×10^{10}*	7.53×10^{-4}
	C	5.17×10^{-3}*	7.88×10^{-3}	1.12	1.10×10^{-2}	1.0*	2.4×10^{13}*	1×10^{10}*	9.16×10^{-8}	1×10^{10}*	6.25×10^{-4}
72.01	R	4.97×10^{-3}	8.75×10^{-3}	1.24	1.23×10^{-2}	0.83	2929*	1×10^{10}*	9.10×10^{-8}*	1×10^{10}*	8.56×10^{-4}
	C	4.97×10^{-3}*	2.48×10^{-3}	3.89	6.93×10^{-3}	1.0*	2929	1×10^{10}*	9.10×10^{-8}	1×10^{10}*	4.66×10^{-4}
80.32	R	7.37×10^{-3}	1.15×10^{-3}	1.17	9.87×10^{-3}	0.78	3474*	1×10^{10}*	1.03×10^{-7}*	1×10^{10}*	5.39×10^{-4}
	C	7.37×10^{-3}*	3.41×10^{-3}	5.51	5.64×10^{-3}	0.74	3474	1×10^{10}*	1.03×10^{-7}	1×10^{10}*	5.38×10^{-4}
96.76	R	5.74×10^{-3}	3.12×10^{-2}	9.23	1.98×10^{-2}	0.66	2213*	1×10^{10}*	1.13×10^{-7}	1×10^{10}*	1.25×10^{-3}
	C	5.73×10^{-3}*	3.52×10^{-2}	13.81	2.95×10^{-2}	0.67	2213*	1×10^{10}*	1.13×10^{-7}	1×10^{10}*	1.94×10^{-3}
102.25	R	1.21×10^{-2}	0.9	14.81*	0.80	0.61	1×10^{12}*	1×10^{10}*	7.78×10^{-8}	1×10^{10}*	7×10^{-3}
	C	1.21×10^{-2}*	0.97*	14.81	0.22	0.68	1×10^{12}*	1×10^{10}*	7.78×10^{-8}*	1×10^{10}*	1.3×10^{-2}

* Denotes values kept constant during iteration.

† R Denotes values obtained from the R equation, C denotes values obtained from the C equation of the computer decomposition.

Table 2. Values of computed circuit components for another new cell

Residual capacity (%)		R_{SOL} (Ω)	θ (Ω)	*CL (F)*	σ ($\Omega s^{-1/2}$)	γ	C_{EXT} *(F)*	R_{EXT} (Ω)	*IND (H)*	R_{IND} (Ω)	*Error* (±)
1.15	R†	1.50×10^{-2}	6.49×10^{-4}	14.97	1.08×10^{-3}	0.52	1147*	1×10^{10}*	8.52×10^{-8}	1×10^{10}*	8.00×10^{-4}
	C†	1.50×10^{-2}*	4.11×10^{-4}	25.34	9.51×10^{-4}	0.5*	1147	1×10^{10}*	7.81×10^{-8}	1×10^{10}*	4.37×10^{-4}
3.64	R	2.59×10^{-2}	1.55×10^{-2}	0.29	2.12×10^{-2}	0.78	398.8*	1×10^{10}*	6.80×10^{-8}	1×10^{10}*	2.03×10^{-3}
	C	2.59×10^{-2}*	5.90×10^{-3}	1.39	1.15×10^{-2}	0.64	398.8	1×10^{10}*	7.16×10^{-8}	1×10^{10}*	3.87×10^{-3}
14.66	R	9.91×10^{-3}	7.06×10^{-4}	5.66	2.56×10^{-3}	0.65	2500*	1×10^{10}*	9.09×10^{-8}*	1×10^{10}*	9.65×10^{-4}
	C	9.91×10^{-3}*	1.21×10^{-3}	2.90	4.22×10^{-3}	0.71	1×10^{12}*	1×10^{10}*	9.09×10^{-8}	1×10^{10}*	1.37×10^{-3}
16.68	R	9.75×10^{-3}	4.05×10^{-4}	1.74	1.84×10^{-3}	0.61	2391*	1×10^{10}*	9.14×10^{-8}	1×10^{10}*	6.05×10^{-4}
	C	9.75×10^{-3}*	5.39×10^{-4}	8.49	1.97×10^{-3}	0.63	2391	1×10^{10}*	7.44×10^{-8}	1×10^{10}*	4.91×10^{-4}
36.71	R	6.85×10^{-3}	1.91×10^{-3}	6.09	3.75×10^{-3}	0.71	2500*	1×10^{10}*	1.01×10^{-7}	1×10^{10}*	7.01×10^{-4}
	C	6.85×10^{-3}*	2.15×10^{-3}	4.66	4.92×10^{-3}	0.73	7250	1×10^{10}*	1.34×10^{-7}	1×10^{10}*	6.16×10^{-4}
48.32	R	1.47×10^{-3}	4.07×10^{-3}	2.86	5.16×10^{-3}	0.76	4000*	1×10^{10}*	9.61×10^{-8}	1×10^{10}*	7.81×10^{-4}
	C	1.47×10^{-3}*	2.68×10^{-3}	4.83	5.17×10^{-3}	0.72	1.82	1×10^{10}*	1.04×10^{-7}	1×10^{10}*	7.16×10^{-4}
61.90	R	5.15×10^{-3}	4.53×10^{-3}	2.53	6.63×10^{-3}	0.83	3393*	1×10^{10}*	9.76×10^{-8}	1×10^{10}*	6.12×10^{-4}
	C	5.15×10^{-3}*	2.34×10^{-3}	4.71	5.45×10^{-3}	0.76	3339	1×10^{10}*	9.76×10^{-8}*	1×10^{10}*	4.72×10^{-4}
67.95	R	5.00×10^{-3}	5.99×10^{-3}	2.24	7.80×10^{-3}	0.85	8125*	1×10^{10}*	9.68×10^{-8}	1×10^{10}*	5.57×10^{-4}
	C	5.00×10^{-3}*	2.76×10^{-3}	5.20	5.54×10^{-3}	0.75	8125	1×10^{10}*	1.01×10^{-7}	1×10^{10}*	3.13×10^{-4}
69.95	R	5.35×10^{-3}	4.03×10^{-3}	4.56	4.98×10^{-3}	0.77	4500*	1×10^{10}*	1.09×10^{-7}	1×10^{10}*	7.22×10^{-4}
	C	5.35×10^{-3}*	2.03×10^{-3}	8.16	4.09×10^{-3}	0.70	5451	1×10^{10}*	1.21×10^{-7}	1×10^{10}*	4.30×10^{-4}
86.01	R	6.82×10^{-3}	1.72×10^{-2}	1.61	1.38×10^{-2}	1.0*	1×10^{12}*	1×10^{10}*	1.16×10^{-7}	1×10^{10}*	9.06×10^{-4}
	C	6.82×10^{-3}*	6.84×10^{-3}	4.61	7.99×10^{-3}	0.81	1.13×10^{4}*	1×10^{10}*	1.15×10^{-7}	1×10^{10}*	4.73×10^{-4}
102.18	R	5.48×10^{-3}	1.07×10^{-2}	10.05	2.29×10^{-2}	0.69	1×10^{12}*	1×10^{10}*	8.86×10^{-8}	1×10^{10}*	1.93×10^{-3}
	C	5.48×10^{-3}*	1.31×10^{-2}	10.09	1.73×10^{-2}	0.68	1×10^{12}*	1×10^{10}*	9.13×10^{-8}	1×10^{10}*	3.44×10^{-3}

* Denotes values kept constant during iteration.
† For definition see footnote to Table 1.

Table 3. Values of computed circuit components for an old cyclon cell

Residual capacity (%)		R_{SOL} (Ω)	θ (Ω)	*CL (F)*	σ ($\Omega s^{-1/2}$)	γ	C_{EXT} *(F)*	R_{EXT} (Ω)	*IND (H)*	R_{IND} (Ω)	*Error* (±)
1.86	R†	3.59×10^{-3}	2.19×10^{-3}	3.31	2.45×10^{-3}	0.5*	2000*	1×10^{10}*	7.84×10^{-7}	2.15×10^{-7}	1.96×10^{-3}
	C†	3.59×10^{-3}*	1.69×10^{-3}	3.37	3.92×10^{-3}	0.5*	1×10^{12}*	1×10^{10}*	7.36×10^{-7}	2.15×10^{-7}*	8.47×10^{-4}
5.36	R	2.49×10^{-2}	7.43×10^{-4}	6.21	2.15×10^{-3}	0.5*	1500*	1×10^{10}*	9.88×10^{-8}	2.27×10^{-6}	2.16×10^{-3}
	C	2.49×10^{-2}*	7.21×10^{-4}	3.59	3.10×10^{-3}	0.5*	1×10^{-12}*	1×10^{10}*	9.13×10^{-8}	2.27×10^{-6}*	3.37×10^{-3}
13.25	R	1.17×10^{-2}	3.30×10^{-4}	20.52	9.40×10^{-4}	0.55	5886*	1×10^{10}*	6.74×10^{-8}	9.04×10^{-2}	8.68×10^{-4}
	C	1.17×10^{-2}	1.00×10^{-4}	32.59	8.26×10^{-4}	0.51	5886	1×10^{10}*	7.35×10^{-8}	9.04×10^{-2}*	7.91×10^{-4}
27.24	R	1.01×10^{-2}	1.92×10^{-4}	37.06	5.08×10^{-4}	0.55	3500*	1×10^{10}*	9.81×10^{-8}	0.65	7.33×10^{-4}
	C	1.01×10^{-2}*	1.47×10^{-4}	34.29	8.53×10^{-4}	0.56	1.53×10^{4}	1×10^{10}*	1.04×10^{-7}	0.65*	6.88×10^{-4}
8.81	R	7.42×10^{-3}	2.70×10^{-4}	21.22	1.23×10^{-3}	0.59	1×10^{12}*	1×10^{10}*	9.44×10^{-8}	2.13×10^{-2}	3.39×10^{-4}
	C	7.42×10^{-3}*	1.92×10^{-4}	13.2	1.95×10^{-3}	0.60	1×10^{12}*	1×10^{10}*	9.88×10^{-8}	2.13×10^{-2}*	4.96×10^{-4}
47.53	R	7.63×10^{-3}	1.57×10^{-3}	6.53	3.44×10^{-3}	0.70	3000*	1×10^{10}*	7.64×10^{-8}	6.31×10^{-2}	4.75×10^{-4}
	C	7.63×10^{-3}	7.20×10^{-4}	12.33	3.27×10^{-3}	0.64	1.69×10^{4}	1×10^{10}*	8.13×10^{-8}	6.31×10^{-2}*	4.75×10^{-4}
52.66	R	6.52×10^{-3}	2.18×10^{-3}	4.54	5.60×10^{-3}	0.75	5000*	1×10^{10}*	7.99×10^{-8}	6.92×10^{-2}	6.38×10^{-4}
	C	6.52×10^{-3}*	6.15×10^{-4}	7.31	5.31×10^{-3}	0.68	8×10^{10}	1×10^{10}*	8.19×10^{-8}	6.92×10^{-2}*	7.07×10^{-4}
68.22	R	6.61×10^{-3}	2.35×10^{-3}	7.14	5.91×10^{-3}	0.74	2500*	1×10^{10}*	1.09×10^{-7}	5.24×10^{-2}	8.30×10^{-4}
	C	6.61×10^{-3}*	1.12×10^{-4}	5.69	6.01×10^{-3}	0.67	1.34×10^{11}	1×10^{10}*	1.09×10^{-7}*	5.24×10^{-2}*	6.00×10^{-4}
78.09	R	7.56×10^{-3}	4.90×10^{-3}	2.74	1.08×10^{-2}	0.88	4769*	1×10^{10}*	9.30×10^{-8}	8.19×10^{-2}	8.71×10^{-4}
	C	7.56×10^{-3}*	5.32×10^{-4}	7.94	5.96×10^{-2}	0.71	4769	1×10^{10}*	1.56×10^{-7}	8.19×10^{-2}*	5.90×10^{-4}
90.135	R	7.71×10^{-3}	1.70×10^{-2}	1.18	2.00×10^{-2}	1.0*	3000*	1×10^{10}*	7.69×10^{-8}	7.62×10^{-2}	7.16×10^{-4}
	C	7.71×10^{-3}*	1.62×10^{-2}	1.37	2.24×10^{-2}	1.0*	1×10^{12}*	1×10^{10}*	7.69×10^{-8}*	7.62×10^{-2}*	5.19×10^{-4}
100.0	R	5.94×10^{-3}	1.29×10^{-2}	2.26	4.17×10^{-2}	0.91	200*	1×10^{10}*	8.19×10^{-8}	8.13×10^{-2}	1.42×10^{-3}
	C	5.94×10^{-3}*	1.21×10^{-2}	1.16	6.46×10^{-2}	1.0*	1×10^{12}*	1×10^{10}*	8.63×10^{-8}	8.13×10^{-2}*	1.71×10^{-3}

* Denotes values kept constant during iteration.
† For definition see footnote to Table 1.

enough with residual capacity to provide a basis for a test. Nor was it possible to find a single frequency determination which provided a satisfactory indication of this quantity even though a careful computer search was made throughout the whole of the available frequency range. This was disappointing, although not altogether unexpected, since we are dealing with development of solid phase $PbSO_4$ at the surface and within the pores of a very complicated and generally undescribed porous structure.

The development of a solid layer of $PbSO_4$ on the surface of an electrode such as PbO_2 reduces the electrode capacitance to a very low value and isolates the electrode from further reaction according to the well described passivation process. Thus the effective areas of the electrodes for the discharging reaction of a lead–acid cell reduced as the discharge proceeded.

Moreover the charge-transfer resistances (per unit area of clean electrode) would be expected to change in time with the reduction of sulphuric acid concentration at reacting centres as the cell is discharged. These factors may be jointly taken into account to a first approximation by considering the product $\theta' C_L$ where $\theta' C_L$ is the effective (experimental) charge-transfer resistance and C_L the effective (experimental) double-layer capacitance.

The relation between the product $\theta' C_L$ and the residual charge for the new and old cells is shown in Fig. 6. Here the values used were obtained from the computer and are corrected for porosity [11]. The product $\theta' C_L$ decreases sharply and smoothly with decreasing residual capacity (RC) in the 50 to 100% range and is thus sufficiently smooth to form the basis of a residual capacity test in this region. It is, however, inconvenient to base a test on a computer decomposition to obtain a product of two basic parameters. If we note that $\theta' C_L$ is the reciprocal of the characteristic frequency for the resistance–capacitance combination and this time constant is readily recoverable from the maximum in the charge transfer semicircle then there

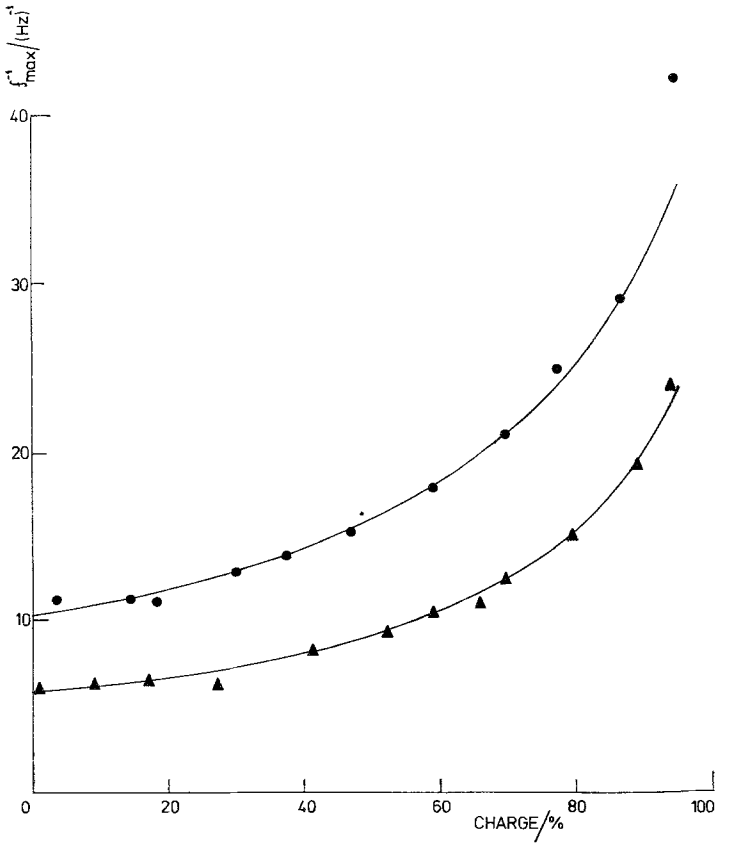

Fig. 7. As Fig. 6, but $\theta' C_L$ obtained directly from the experimental impedance from the reciprocal of the frequency at the top of the high frequency semi-circle, for (●) new and (▲) old cells.

is a simple method of finding the product. The question naturally arises as to whether or not the local maximum in the experimental charge-transfer semicircle can be identified. Fig. 7 shows the product $\theta' C_L$ obtained by spotting the maximum in the experimental impedance plotted against residual capacity for both new and old cells. If anything the data are more useful than those originating from the computer and clearly provide an excellent estimation in the residual capacity range 50 to 100%. A two to four fold increase in magnitude of the index occurs as the residual charge increases from 0 to 100%.

Another noteworthy feature of this work is that a basic difference is observed with differently aged and differently treated cells. This feature forms the basis of a 'state-of-health' test for lead–acid cells. It is reasonable to suppose that the large number of charge/discharge cycles undergone by the cell produces 'wear' of the positive plates with the generation of more fine particles and an attendent increase in double-layer capacitance. This is qualitatively what is observed here, an increase in effective plate area is a satisfactory explanation of the effects observed and an increase in the general level of $\theta' C_L$.

It is not desirable to use the extensive equipment described in this study as an onboard test for an aircraft battery due to space and weight. The specific onboard test for an aircraft battery for example cannot tolerate the necessity of a large amount of equipment inherent in our harmonic test procedure. We can now achieve a complete test via the isolation of the time constant in a few seconds using fast noise and Fourier methods.

Acknowledgement

This work was carried out with the support of Procurement Executive, Ministry of Defence.

References

[1] S. A. G. R. Karunathilaka, N. A. Hampson and R. Leek, *Surface Technol.* **13** (1981) 339.
[2] N. A. Hampson, S. A. G. R. Karunathilaka and R. Leek, *J. Appl. Electrochem.* **10** (1980) 3.
[3] S. A. G. R. Karunathilaka, N. A. Hampson, T. P. Hass, R. Leek, T. J. Sinclair, *ibid.* **11** (1981) 573.
[4] M. Hughes, R. T. Barton, S. A. G. R. Karunathilaka, N. A. Hampson and R. Leek, *ibid.* **15** (1985) 129.
[5] W. G. Marshall, R. Leek, N. A. Hampson and G. Lovelock, *J. Power Sources* **13** (1984) 75.
[6] S. A. G. R. Karunathilaka, R. T. Barton, M. Hughes and N. A. Hampson, *J. Appl. Electrochem.* **15** (1985) 251.
[7] J. Bialacki, N. A. Hampson and J. Pearson, *Surface Technol.* **23** (1984) 117.
[8] N. A. Hampson, S. Kelly and K. Peters, *J. Appl. Electrochem.* **11** (1981) 751.
[9] S. Cotgreave, N. A. Hampson and S. A. G. R. Karunathilaka, Interim Report to MoD Contract No. ER/a/9/4/2170.095/RSRE.
[10] N. A. Hampson and M. J. Willars, *Surface Technol.* **7** (1978) 247.
[11] R. de Levie in "Advances in Electrochemical Engineering" Vol. 6, edited by P. Delahay, Interscience, New York (1967) p. 329.
[12] H. A. Laitinen and J. E. B. Randles, *Trans. Faraday. Soc.* **51** (1955) 54.
[13] S. Kelly, N. A. Hampson and S. A. G. R. Karunathilaka, *Surface Technol.* **13** (1981) 349.